

# Numerical simulation study on the heat transfer of a spiral tube receiver designed to a thermal power tower.

Toufik Arrif \*, Abdelfettah Belaid, Amor Gama,  
and Rida Zarrit

Unité de Recherche Appliquée en Energies  
Renouvelables, URAER, Centre de  
Développement des Energies Renouvelables, CDER, 47133,  
Ghardaïa, Algeria  
\*arriftou@yahoo.fr

Abdelmadjid Chehhat  
Faculty of Science and Technology  
University Laghrour Abbess  
Khenchela, Algeria  
achehhat@gmail.com

**Abstract**— in this work the heat transfer of a spiral tube receiver exposed to concentrated solar radiation is studied theoretically. The simulations were performed using *Fluent6.3.26* for two different sections at several Reynolds numbers: 100, 300, 500, 700, and 1000 to see the effect of the inlet velocity on the outlet temperature. The effect of the inlet temperature is also discussed by varying the inlet temperature of the water of 293K to 313K. The results show that the average temperature of the heating and adiabatic surface (inner wall) is decreasing when the velocity inlet is increasing. The outlet temperature of a semicircular section is higher than that of the circular section, but the *Nusselt* number of this one is twice higher as that of semicircular section and it's due to the geometrical shape of the section.

**Keywords**- Key words: heat exchanger, heat transfer, spiral tube

## I. INTRODUCTION

In a solar thermal power tower system, the cylindrical receiver (heat exchanger tube) is a key component for solar concentration system. The average temperature of the inner wall of the tube is an important operating parameter [1]. The main obstacle to the development of solar tower technology is the significant investment required by the construction of a field of heliostats and tower. Naphon [2] studied the characteristics of the heat transfer and flow of a horizontal spiral coil tube by numerical and experimental method.

In actual solar thermal power, because of the different concentrated solar radiation and different incident angle, the heat transfer is uneven along the circumference. The local temperature, heat flux and heat transfer coefficient of the tube

receiver need to be obtained when the solar plant operates normally [3].

Concerns the solar heat exchanger fluid (water/solar) high temperature we designed a spiral tube geometry with two variable sections. The aim is to seek optimum designs of spiral ducts for solar applications where the cross section area is fixed. The computational domains in Figures 7 and 8 were created in *GAMBIT (2.3. 16)* software then simulated in *FLUENT (6.3.26)* and then will be integrated and simulated in *TRNSYS*. The solar receiver (heat exchanger) presented in this work consists of one single spiral tube arranged vertically. In this study we simulate heat transfer spiral tube operating with water as the working fluid and one half circumference of the tube receiver receives the solar radiation energy, and the second half is supposed adiabatic surface covered with heat insulator. To compare the two geometries, numerical simulations were carried out for fixed cross section area and pipe length. The results of numerical simulations in this document show the particular distribution of *Nusselt* number and temperature.

## II. MODEL DEVELOPMENT

In this study, incompressible laminar Newtonian fluid flows inside a spiral duct with two cross sections is taken into account. The configurations of in-plane spiral ducts and their respective cross section schematic are displayed in Fig.1and 2; the detailed geometric parameters are presented in Table I. In this work we consider one side of tube called the heating surface receives constant heat flux from the solar radiation  $Q_{Net} = 10000 \text{ W/m}^2$ , and the other side is called adiabatic surface

covered with heat insulator. Fig. 2 shows coordinate system and thermal boundary conditions.

The water enters through the spiral pipe with the velocity and the temperature inlet  $U_{in}$  and  $T_{in} = 303$  K, it absorbs heat and its temperature increases, and exits and flows through the outlet, in this study the properties of the water are constant. Conservation equations for mass, momentum and energy for the flow inside the ducts are given by [4], [7]:

$$\nabla \cdot \rho u = 0 \tag{1}$$

$$\nabla \cdot (\rho u \cdot u) = -\nabla p + \nabla [\mu(\nabla u + (\nabla u)^T)] \tag{2}$$

$$\rho c_p \cdot \nabla(u \cdot T) = k \nabla^2 T \tag{3}$$

$\rho$ : Density of liquid water,  
at  $30^\circ\text{C}$  :  $\rho$  (kg/m<sup>3</sup>)= 995.6502

$u, v, w$ : fluid Velocity in  $xyz$

$P$  : pressure, pas

$\mu$  : fluid dynamic viscosity

$C_p$ : Constant-pressure heat capacity  
at  $30^\circ\text{C}$  :  $CP$  (J/(g·K))= 4.1784

$K$ : thermal conductivity of the fluid  
 $K$  [W·m<sup>-1</sup>·K<sup>-1</sup>]=0.609

$T$ : temperature.

Table I Dimensions of the spiral tube.

Parameters	Dimensions (mm)	
	circular Section	semi circular Section
Inner diameter of tube, d	20	28
Innermost spiral tube diameter,	140	140
Outermost spiral-coil tube diameter ,	680	720
Length of spiral tube,	6365	6365
Pitches,	30	30
Number of coil turns,	5	5

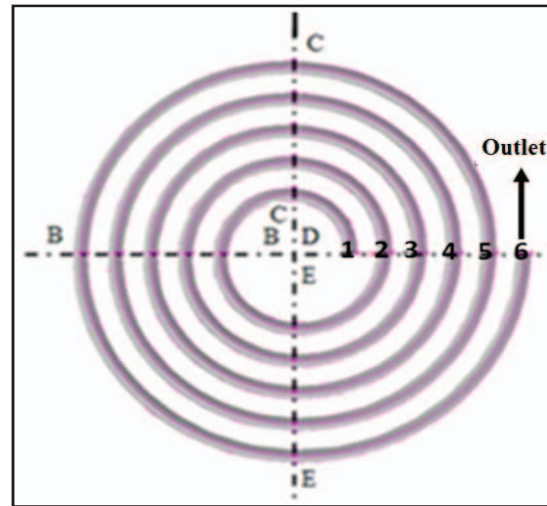


Fig. 1 Schematic diagram of the spiral tube.

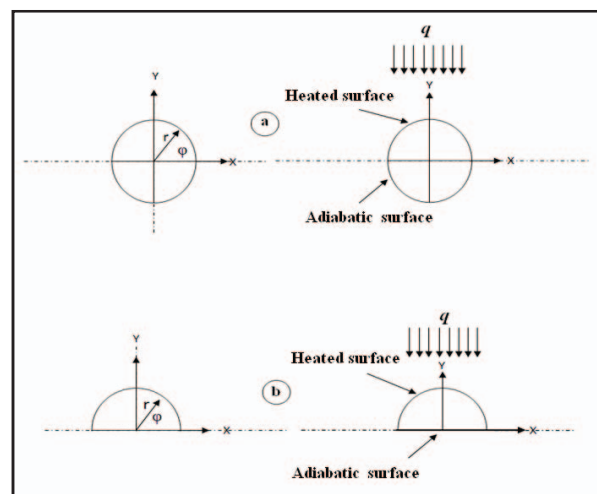


Fig.2 Schematic of coordinate system and thermal boundary conditions: a) circular section, b) semi-circular section.

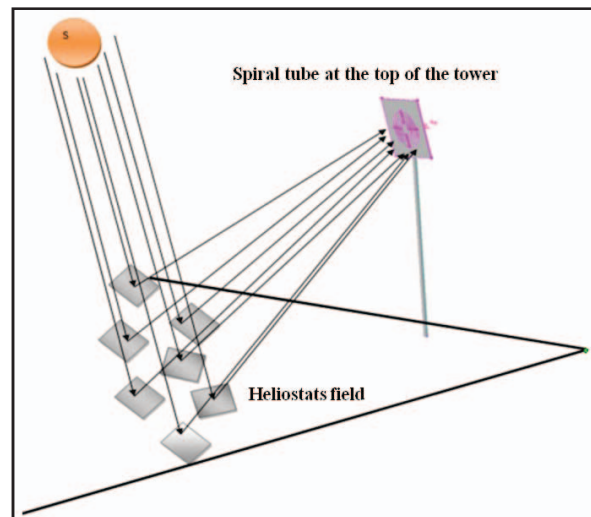


Fig.3. Simplified representation of the solar tower.

### III. BOUNDARY CONDITIONS AND NUMERIC COMPUTATION:

*GAMBIT* (2.3.16) is used to mesh the two geometries shown in Figure 4 with a Tetrahedron volume element. The boundary definitions are *VELOCITY INLET* for inlet boundary, *OUTFLOW* for outlet boundary, *WALL* for other boundaries, *FLUID* for water in the tube, and *SOLID* for tube wall.

The mathematical model given by Equations. (1)– (3), together with appropriate boundary condition and constitutive relations comprising five dependent variables –  $u$ ,  $v$ ,  $w$ ,  $P$  and  $T$  – was solved using the commercial code *Fluent 6.3.26* based on finite volume method. *SIMPLEC* algorithm is employed to deal with the problem of velocity and pressure coupling *Van Doormal* and *Raithby* (1984) [5], the steps of this algorithm are almost the same as the *SIMPLE* algorithm with the difference that he neglect least significant terms in the velocity correction equations. Second-order upwind scheme and tetrahedral grid are used to discretize the main governing equations as shown in Fig. 4. The numerical computation is ended if the residual summed over all the computational nodes satisfies the criterion  $10^{-4}$  except for energy equation criteria for residual is  $10^{-6}$ , (fig 7).

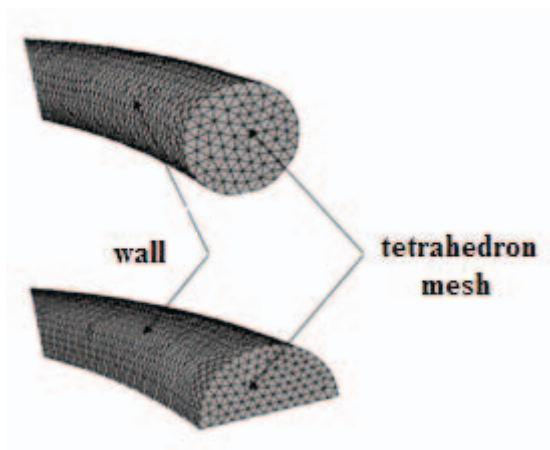


Fig.4 Schematic diagram of the tetrahedron grid system for spiral tube.

#### A. Grid independence :

In order to obtain the satisfactory solutions, the grid independence is carried out in the analysis by comparing the temperature at the outlet of the spiral tube to the diameter of this one.

( $-r < Y < r$ ,  $X = 0.33$ ,  $Z = 0$ ) for circular section.

( $0 < Y < r$ ,  $X=0.37$ ,  $Z=0$ ) for semicircular section.

1) *circular section*: A different grid distributions of 226823, 401967 and 511366 was tested and it indicated that all the grid have identical temperature profiles. We choose to

use later in our calculations the amount of grid 226.823 as it ensures a satisfactory solution.

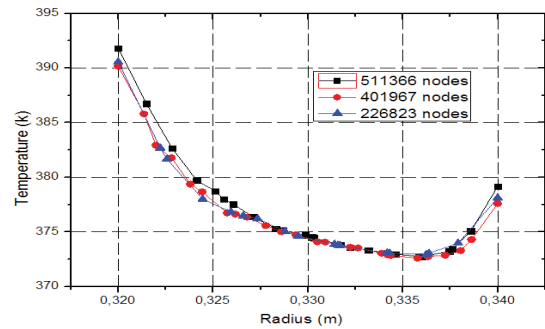


Fig.5 Test of Grid independence for circular section:  $Re = 500$ ,  $T_{in} = 303k$ .

2) *Semi circular section*: A different grid distribution of 256042, 338347, 463150 and 526474 was tested and it indicated that all grid distributions have identical temperature profiles. So for the half circular section we choose a grid of 256.042 as it ensures a satisfactory solution and it does not consume time.

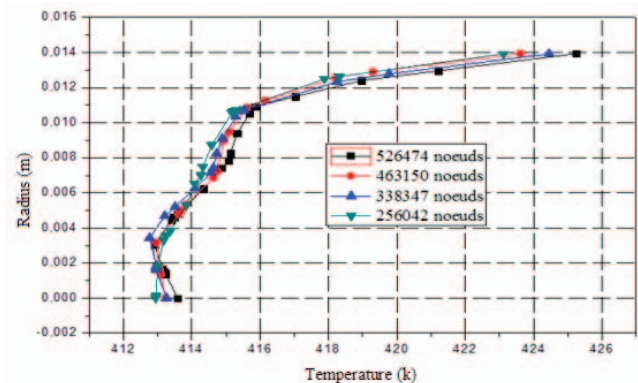


Fig.6 Test of Grid independence for semi circular section:  $Re = 500$ ,  $T_{in} = 303k$ .

### IV. RESULTS AND DISCUSSION:

In order to evaluate the performance of heat transfer in spiral tubes exposed to a concentrated heat flux, numerical simulations were carried out for two different sections. The cross-sectional area is fixed so we can observe the effects of different cross sections in the flow.

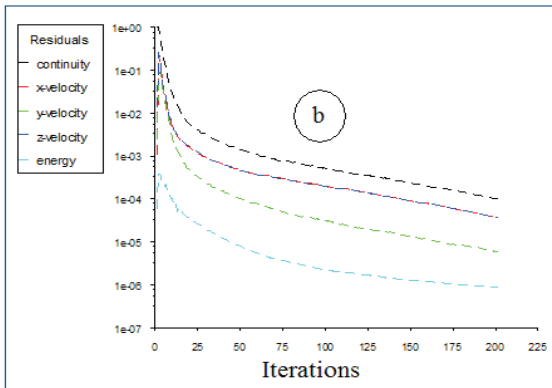
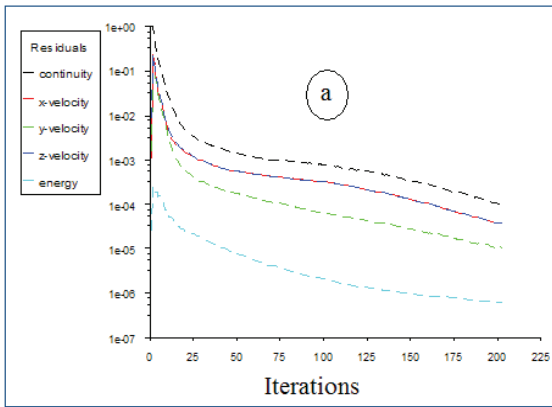


Figure.7. Evolution of residuals: (a) circular section (b) semi-circular section.

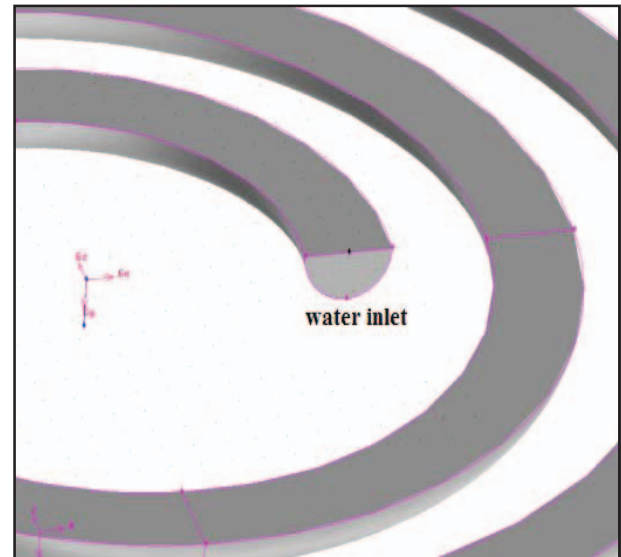


Figure.8 Computational domain: (a) circular section (b) Semi-circular section.

A. *Température :*

Figures 9 and 10 show the temperature distribution which is uneven in the Y direction, and that the outlet temperature of the half circular section tube is higher than the circular cross-section and maybe it is due to the geometric shape section. According to previous studies [6], the presence of the centrifugal force due to the curvature of the spiral induces a large radial pressure gradient in the central region of the flow.

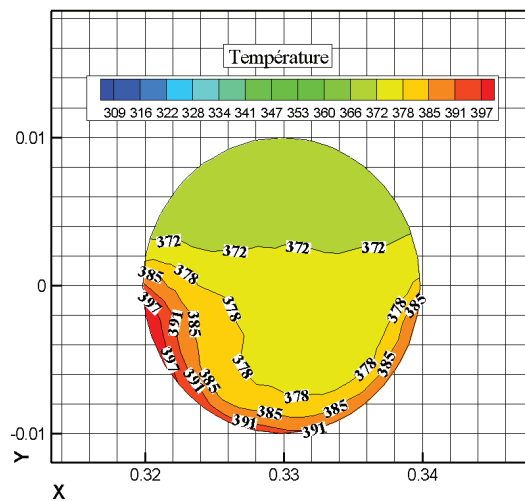
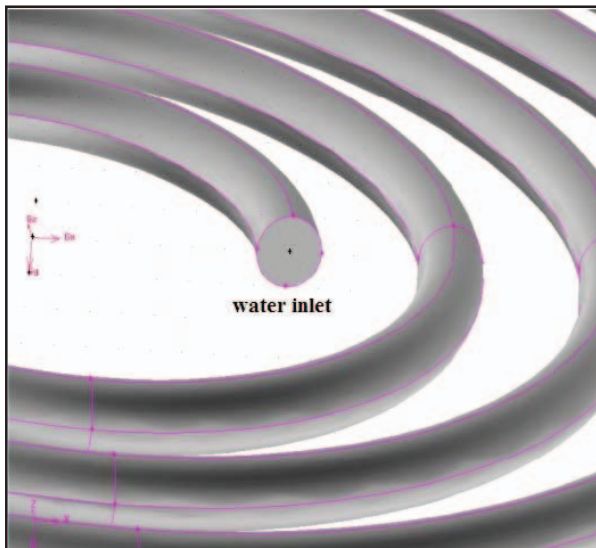


Fig.9 Temperature Distribution, circular section, section DD (Re = 500, Tin = 303k, outlet tube).

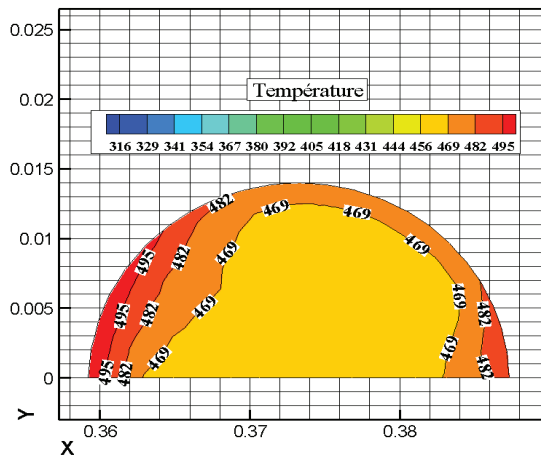


Fig.10 Temperature Distribution, half circular section, section DD (Re = 500, Tin = 303k, outlet tube).

As a result of centrifugal force on the temperature distribution as shown in Figures 11, 12, 13 and 14, the maximum temperature is observed in the outer side away from the inlet section up to 400k for the circular cross section and 495 for the semi circular cross section. This result has a significant effect on improving the heat transfer between the working fluid in the center of the tube and the working fluid near the tube wall.

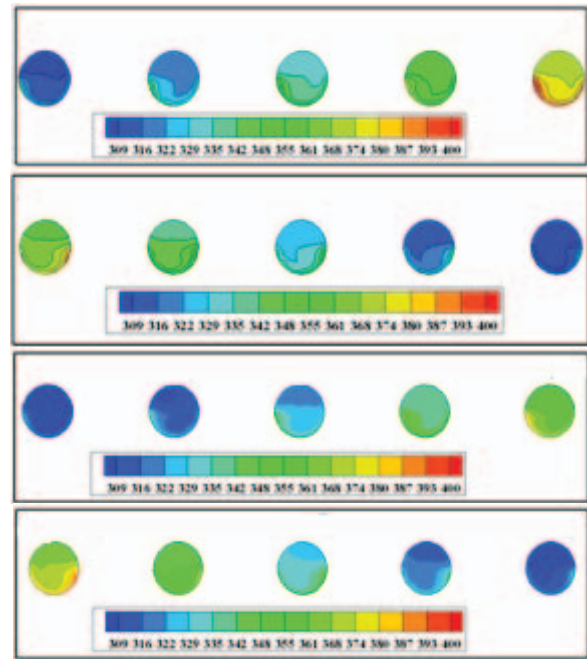


Fig.12 Temperature profile for different sections, Re = 500, Tin = 303k (circular sections).

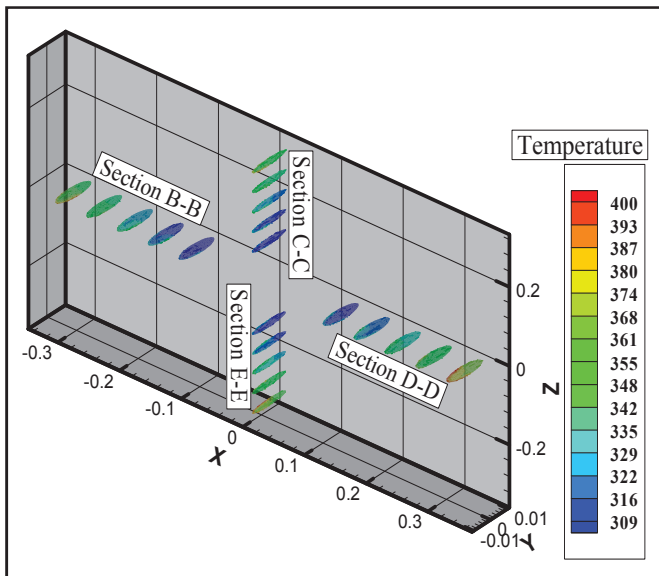


Fig.11 3D view of the temperature distribution in various sections of the spiral tube (receiver), circular Section.

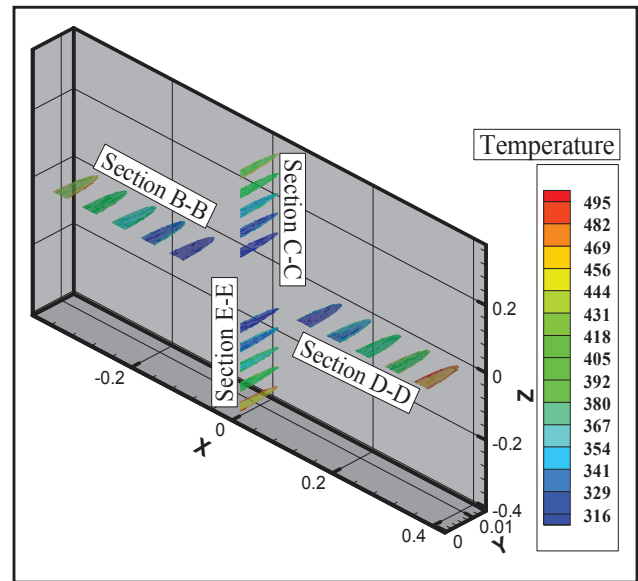


Fig.13 3D view of the temperature distribution in various sections of the spiral tube (receiver), semicircular Section.

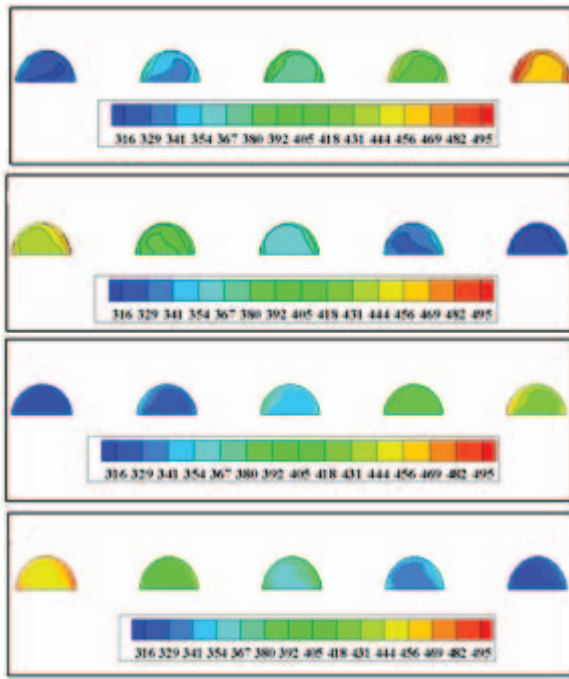


Fig.14 Temperature profile for different sections, Re = 500, Tin = 303k (Semi-circular Sections)

surface is very high, reaching 720 K and 1150 K for semi-circular and circular section respectively. As the velocity increases, the temperature of the inner wall gradually decreases, and the difference of temperature between the heated and adiabatic surface becomes lower, thus increasing the velocity increases the heat transfer of the adiabatic surface and tends to balance temperature, which reduces the temperature of the inner wall of the tube.

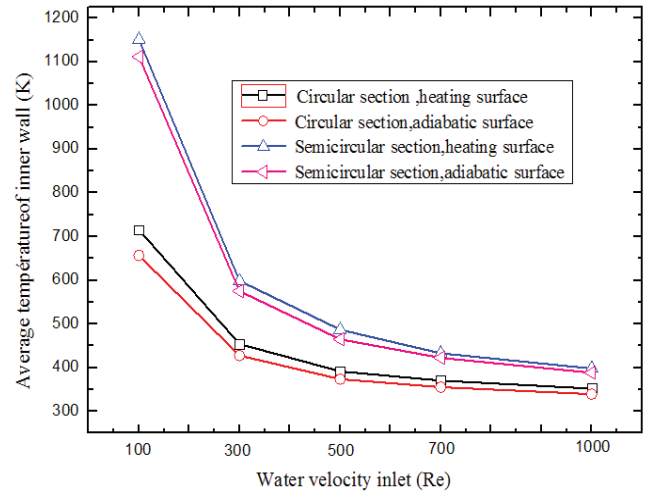


Fig.16 The average temperature of inner tube wall at different inlet velocity. (T in=303k).

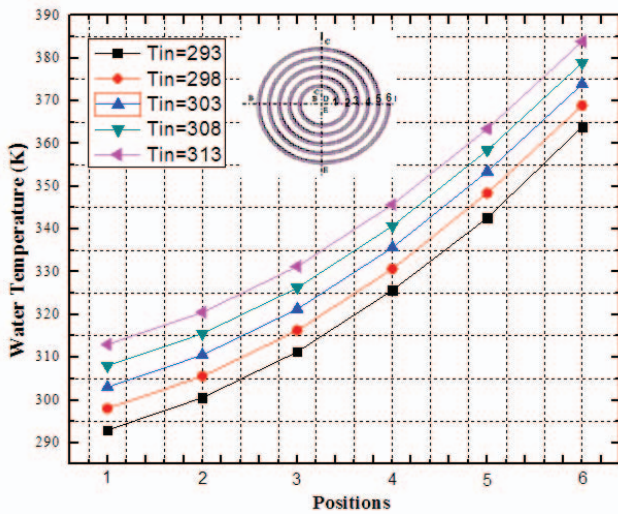


Fig.15 Variation of water temperature with position of spirally coiled tube. (Circular cross section, Re = 500).

Figure.15 represents the variation of the water temperature with the position along the spiral tube (circular cross section) for different inlet temperature. Positions 1 and 6 are input and output of the vertical spiral respectively. Water temperature increases with increasing of distance from the inlet to outlet and the highest value is 385k for Tin = 313k.

Figure 17 shows the change in average temperature of the inner wall of the tube at different input velocity. When water velocity is low (Re = 100), the temperature of the heated

**B. Nusselt number :**

In general, the coefficient of heat transfer through the fluid can be found by the formula [1]:

$$Nu = h.d / K ; \text{ et } q = h. (t_w - t_f), \tag{4}$$

Nu: Nusselt number

q : heat flux

t<sub>w</sub> : inner wall tube temperature.

t<sub>f</sub> : fluide average Temperature.

h : convective heat transfer coefficient

The water Prandtl number under laminar flow at temperature T<sub>in</sub>= 303k is [7]:

$$Pr = \frac{v}{\alpha} = 5.43 \tag{5}$$

Pr : prindlt number

v : water cinematic viscosity at 303k : v= 0.804x10<sup>-6</sup> m<sup>2</sup>/s

α : thermal diffusivity m<sup>2</sup>/s (α=K /ρ .C<sub>p</sub>)

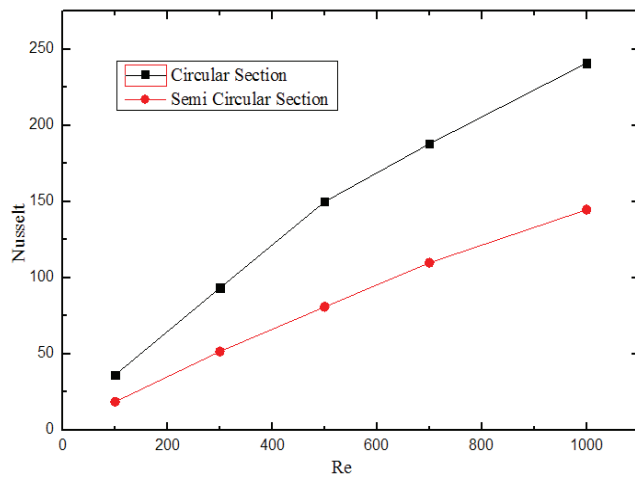


Fig.17 Variation of Nusselt number with Reynolds number  
( $T_{in} = 303k$ , output tube)

Figure 18 shows the variation of the *Nusselt* number with *Reynolds* number for the same simulation conditions, it increases with the increase in velocity, *Nusselt* number of the circular section is higher than semi circular section (1 times higher), thus the geometry of the section of the tube influences *Nusselt* number.

#### V. CONCLUSION

In this work we have designed two three-dimensional geometries with *GAMBIT 2.3.16* software, one has a circular cross section and the second has semi-circular cross section, the three-dimensional water laminar flow was simulated with *FLUENT 6.3.26* commercial code that is based on the finite

volume method in order to analyzing the characteristics of the heat transfer and flow numerically. These two geometries were imagined in order to be used for exchanger fluid / solar in a solar tower.

We introduced a comparison between two different cross sections of a spiral tube; it was found that the outlet temperature of the spiral semicircular cross section is higher than the circular one. The temperature difference between the two heated and adiabatic faces decreases with increasing velocity. The cross section geometry of the tube influences the outlet temperature and the *Nusselt* number of the fluid.

#### REFERENCES

- [1] Xiaoping Yang ,Xiaoxi Yang, Jing Ding,Youyuan Shao , Hongbo Fan,," Numerical simulation study on the heat transfer characteristics of the tube receiver of the solar thermal power tower" *Applied Energy*, vol. 90, issue 1, pp. 142-147, 2012.
- [2] Naphon Paisarn. 'Study on the heat transfer and flow characteristics in a spiral- coil tube'. *Int Commun Heat Mass Transfer* vol 38: pp. 69-74, 2011.
- [3] S.Vashisth, V.Kumar, K.D.P.Nigam, A review on the potential applications of curved geometries in process industry, *Ind.Eng.Chem.Res.* vol 47, pp. 3291-3337,2008.
- [4] Reilly HE, Kolb W J. 'Evaluation of molten salt power tower technology based on The experience of solar two '.SANDIA Report SAND -3674, 2001.
- [5] Agus P.Sasmito et al. 'Numerical analysis of laminar heat transfer performance of in-plane spiral ducts with various cross-sections at fixed cross-section area'. *International Journal of Heat and mass Transfer* Vol 55, Issues 21-22, pp.5882-5890, October 2012.
- [6] Patankar, S.V. 'Numerical heat transfer and fluid flow', hemisphere publishing corporation Taylor and Francis group, New York (1980).
- [7] W. Kays, M. Crawford, B. Weigand, *Convective Heat and Mass Transfer*, fourth ed., McGraw-Hill, Singapore, 2005.